



HAL
open science

Rarefied gas flows in softwood tracheid network: identification of morphological parameters from gas permeability measurements

Ai Wei, Hervé Duval, Florian Pierre, Patrick Perré

► **To cite this version:**

Ai Wei, Hervé Duval, Florian Pierre, Patrick Perré. Rarefied gas flows in softwood tracheid network: identification of morphological parameters from gas permeability measurements. 2nd European Conference on Non-equilibrium Gas Flows – NEGF15, Dec 2015, Eindhoven, Netherlands. hal-01809858

HAL Id: hal-01809858

<https://hal.science/hal-01809858>

Submitted on 14 Jun 2018

HAL is a multi-disciplinary open access archive for the deposit and dissemination of scientific research documents, whether they are published or not. The documents may come from teaching and research institutions in France or abroad, or from public or private research centers.

L'archive ouverte pluridisciplinaire **HAL**, est destinée au dépôt et à la diffusion de documents scientifiques de niveau recherche, publiés ou non, émanant des établissements d'enseignement et de recherche français ou étrangers, des laboratoires publics ou privés.

DRAFT NEGF15-23

**RAREFIED GAS FLOWS IN SOFTWOOD TRACHEID NETWORK:
IDENTIFICATION OF MORPHOLOGICAL PARAMETERS FROM
GAS PERMEABILITY MEASUREMENTS**AI Wei¹, DUVAL Hervé¹, PIERRE Florian¹, PERRÉ Patrick¹¹Laboratoire de Génie des Procédés et Matériaux, CentraleSupélec, Université Paris Saclay, Grande
Voie des Vignes, 92295 Châtenay-Malabry, Francewei.ai@centralesupelec.fr, herve.duval@centralesupelec.fr, floran.pierre@centralesupelec.fr,
patrick.perre@centralesupelec.fr**KEY WORDS**

wood, multiscale porous media, rarefied gas flow, apparent permeability, parallel and series microchannel systems, parameter identification.

ABSTRACT

We propose a new method to identify morphological parameters of porous (bio)materials. This method is based on gas apparent-permeability measurements and takes advantage of the flow regime changes which occur at different pressure depending on the pore size.

The apparent permeability at a given mean pressure is measured from the pressure relaxation kinetics when gas is allowed to permeate through the tested material from a slightly higher pressure compartment to a slightly lower pressure one. Our set-up is able to measure apparent permeability ranging from 10^{-10} to 10^{-18} m².

Then, morphological parameters are identified from the variations of apparent permeability as a function of the mean pressure, thanks to a pore network model. The network consists in elements such as pipes, slits or orifices connected in series or in parallel. The unknowns may be the connectivity of the network, the duct diameter or the slit width for example. The flow in each element is described by the appropriate model. The unknowns are determined by minimizing the deviation between the experimental variations of the apparent permeability and the simulated ones.

The present approach is first applied to track-etched polycarbonate membranes. It appears that the identified pore radius is of 38 nm, close to the measured value by scanning electron microscopy equal to 35 nm. Then, Norway spruce is tested: the identified mean pit radius and pits number per tracheid in both tangential and longitudinal direction are in reasonable agreement with anatomical data reported in literature

1. INTRODUCTION

Wood is an example of smart natural microfluidic system. In live softwood, sap is transported through microscale elongated cells called tracheids which run lengthwise with trunk and are interconnected via smaller orifices called bordered pits. In dry wood, transport properties, in particular gas permeability, mainly rely on the tracheid network.

Wood multiscale porosity may be characterized by serial cross-section analysis or micro-tomography. However, the nanoscale porosity such as the inter-tracheid pits remains difficult to be accessed with such methods.

In the present study, we revisit an alternative approach based on the analysis of the gas apparent-permeability variations as a function of the gas pressure [1]. The idea consists in taking advantage of the flow regime changes (typically from Darcy's flow to slip flow), which occur at different mean pressures depending on the pore size, in order to identify pore-network characteristics.

The permeability of dry wood ranges over several orders of magnitude, *i.e.* from 10^{-10}m^2 (red-oak in longitudinal direction) to $3\times 10^{-21}\text{m}^2$ (Spotted gum in tangential direction [2]) depending on the species, on the position (heartwood is always less permeable than sapwood) and on the direction since wood is strongly anisotropic.

In the following, we first present the experimental device specifically designed to measure a wide range of permeability. Then, we report measurements carried out on a well-defined porous material, *i.e.*, polycarbonate track-etched membrane, and on a well-documented softwood species, *i.e.*, Norway spruce. Last, the identification approach is presented and applied to these experimental results.

2. MATERIALS AND METHODS

2.1 Sampling

Two types of porous materials have been examined, *i.e.*, ultrafiltration membranes and Norway spruce. The membranes are commercialized track-etched polycarbonate membranes (KN5CP81030, supplied by GE Osmonics). These membranes are symmetric and have controlled cylindrical pores. The pore nominal radius is equal to 25 nm, the mean pore density to 6×10^{12} pores $\text{m}^{-2} \pm 15\%$ and the membrane thickness to $6\mu\text{m} \pm 10\%$ as specified by the supplier. Disc samples with a diameter of 47 mm were cut from membrane sheet and used for the permeability measurements.

The Norway spruce was cut from Risoux forest in the east of France. Wood specimen were dried under natural condition. The tested material had an average basic wood density (oven-dry mass to green volume) of $360\text{ kg}\cdot\text{m}^{-3}$. Defect-free Norway spruce samples were cut from the heartwood part of the wood log (Fig.1). Sampling was performed in two directions, *i.e.*, longitudinal and tangential. Note that the shape of the samples has been adapted to the wood permeability in the associated direction. Hence, in the longitudinal direction, characterized by high permeability values, rod sample with a diameter of 18 mm and a thickness of 30 mm were cut. On the contrary, in the tangential direction, characterized by low permeability values, disc sample with a diameter of 72 mm and a thickness of 10 mm were cut. Last, the lateral surface (parallel to the sampling direction) of the wood samples were systematically coated with epoxy resin in order to obtain a smooth impermeable surface.

2.2 Scanning electron microscopy

The structure of the porous materials were characterized by scanning electron microscopy (SEM). The track-etched membranes were observed with a field emission scanning electron microscopy (LEO 1530) after deposition of a 5 nm thick tungsten film (using a PECS, Precision Etching Coating System, from Gatan). The micrographs were analyzed using the public domain software ImageJ [3] in order to determine the pore size distribution and the mean pore density of the membranes. The measured mean pore radius is equal to 35 nm with a mean standard deviation of 5 nm. The measured mean pore density is equal to $6.5 \pm 0.2\times 10^{12}$ pores m^{-2} . The measured membrane thickness is equal to $6.5 \pm 0.4\mu\text{m}$. These values are in good agreement with GE Osmonics specifications.

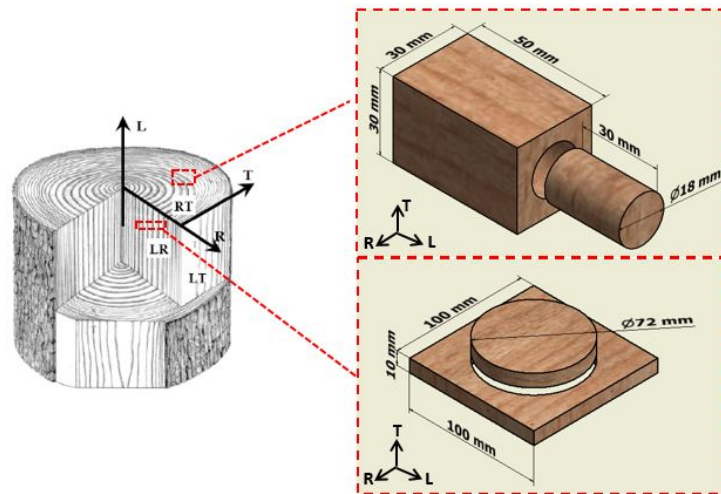


Figure 1: Wood sampling in the longitudinal (L) and tangential (T) directions.

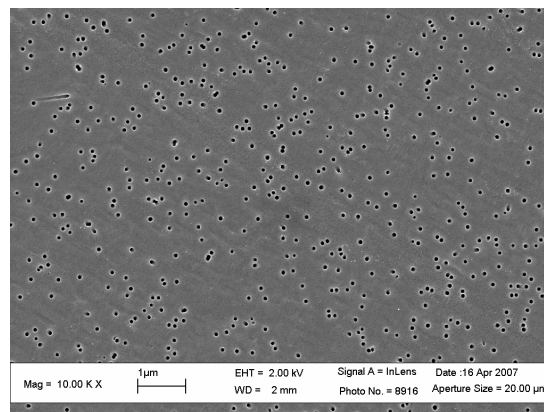


Figure 2: Micrograph of a track-etched polycarbonate membrane by SEM (KN5CP81030, GE Osmonics).

The Norway spruce specimen were observed with an environmental scanning electron microscope (ESEM, FEI Quanta 200). The samples were carefully cut using a microtome after a two-days immersion in distilled water. Then, they were dried under natural conditions before being observed by ESEM. We found that the tracheid mean radius is equal to 11.7 μm with a standard deviation of 4.8 μm . It should be noted that the large standard deviation is due to the simultaneous presence in one sample of two types of wood with different characteristics, *i.e.*, early wood and late wood. In the early wood, the tracheids are larger, *i.e.*, 14.8 μm with a standard deviation of 1.9 μm . In the late wood, tracheids are narrower, *i.e.*, 4.3 μm with a standard deviation of 1.4 μm . The radius of the bordered pits (see Fig. 3, left) is estimated at 0.7 μm with a standard deviation of 0.08 μm .

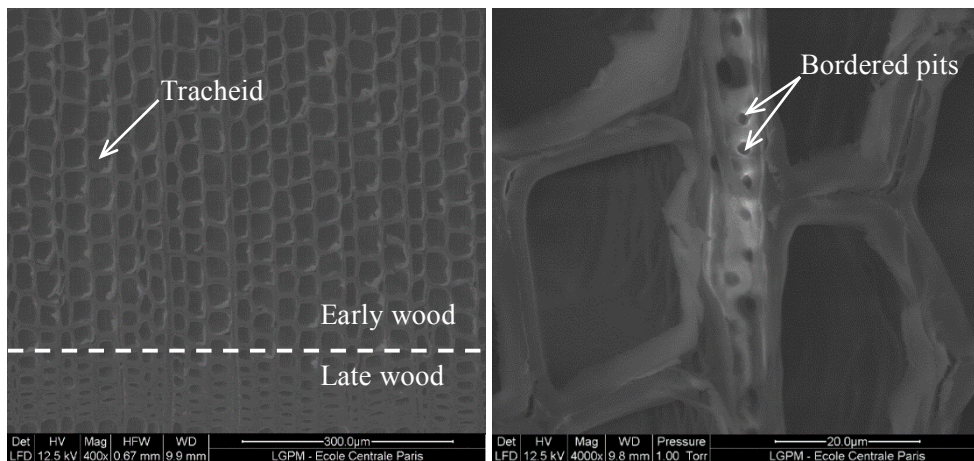


Figure 3: Micrographs of Norway spruce by ESEM: tracheid assembly (left) and zoom on bordered pits (right).

2.3 Experimental apparatus

A specific device, inspired by Agoua and Perré [5], was designed to measure a wide range of permeability. The principle of the permeability measurement consists in imposing a pressure difference on either side of the tested sample and determining its permeability from the pressure relaxation kinetics.

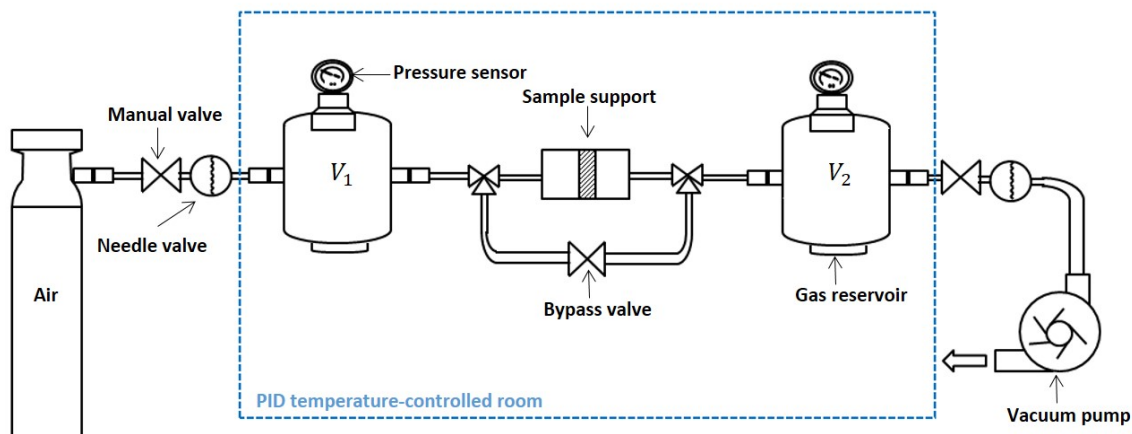


Figure 4: Experimental device.

The device (see Fig. 4) is composed of two identical gas chambers tightly connected via a sample support. The support can be isolated from the chambers through two slide vacuum valves. The gas pressure in the chambers is measured by highly sensitive pressure sensors (GE Druck, TERPS RPS/DPS 8000). The pressure range of the sensors extends from about 0 to 2000 mbar with a precision of 0.2 mbar between 35 mbar and 2000 mbar at 25 °C . The capacity V_{ch} of the chambers (from 0.01 L to 24 L), the dimensions of the sample (thickness L from a few micrometers to 30 mm) and the support geometry are adjusted depending on the permeability range of the sample in order to optimize the measurement accuracy. The entire device is put in a PID temperature-controlled room. The experimental protocol consists in setting the two chambers at different but neighboring pressures and in measuring the pressure relaxation in the chambers when gas is allowed to permeate through the sample from the high pressure chamber to the low pressure one. The pressure variations in both chambers are recorded as a function of time. Experiments are carried out for different initial mean pressures.

3. RESULTS

3.1 Pressure relaxation

Typical examples of pressure relaxation curve as a function of time are reported in Fig. 5, for track-etched polycarbonate membrane and Norway spruce in the longitudinal and tangential directions, respectively. It can be seen that the pressure of each chamber, *i.e.* P_1 (high pressure chamber) and P_2 (low pressure chamber), relaxes toward the mean pressure $P_m = (P_1 + P_2)/2$ since the gas chambers have the same volume.

The duration of an experiment may vary over several orders of magnitude : from 100 seconds in the case of a thin track-etched membrane to 10^5 s for low permeable materials. In the latter case, the initial pressure difference between the chambers is increased from about 10 mbar to about 100 mbar in order to get reasonable experiment duration and pressure relaxation kinetics large enough compared to the “intrinsic” leak rate of the set-up. We measured the intrinsic leak rate at the lowest mean pressure of our experiments (using a “perfectly” impermeable sample) : the leak rate is of 0.2 mbar/hour at mean pressure of 30 mbar for the smallest chambers and is of 0.7 mbar/hour at mean pressure of 30 mbar for the largest ones. These values remain much lower than the pressure relaxation rates measured in the present experiments.

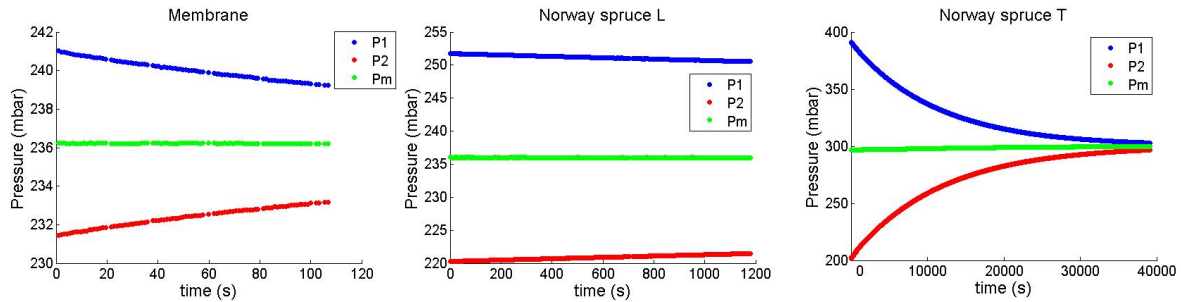


Figure 5: Pressure relaxation in the chambers for the track-etched membrane (left) and the Norway spruce specimen in the longitudinal direction (center) and in the tangential direction (right).

In the left graph of Fig. 5 (Norway spruce in tangential direction), the pressure relaxation through the sample is almost complete. Although complete relaxation is not necessary to access apparent permeability, this experiment shows that the relaxation curves look like exponential. Furthermore it can be seen that the intrinsic leak rate of the set-up remains low throughout this long experiment.

3.2 Apparent permeability

The apparent permeability, K_{app} , is defined as:

$$\frac{Q(x, t)}{A_s} = - \frac{K_{app}}{\mu_0} \frac{dP}{dx} \quad (1)$$

where Q is the gas volume flow rate flowing across the sample, A_s is the sample cross-section area, μ_0 is the dynamic viscosity of air at the room temperature and dP/dx is the pressure gradient in the direction of the mean flow.

We express the volume flow rate as a function of the molar flow, the temperature and the gas pressure using the ideal gas equation of state and we integrate Eq. (1) under the quasi-steady state assumption, from $x = 0$ to $x = L$ where L is the sample thickness. We get:

$$K_{app} = \mu_0 \frac{Q(x, t) L}{A_s(P_1(t) - P_2(t))} \frac{P(x, t)}{P_m} \quad (2)$$

where $P_m(t) = (P_1(t) + P_2(t))/2$.

If we assume that the relaxation is slow enough to be isothermal, the gas volume flow rate may be expressed as:

$$Q(t) = V_{ch} \frac{dP_1(t)/dt}{P_1(t)} \quad (3)$$

where P_1 is the pressure in high pressure chamber and V_{ch} the volume of a chamber.

Under the isothermal assumption, the pressure relaxation in the two identical gas chambers are equal but opposite:

$$\frac{dP_1(t)}{dt} = -\frac{dP_2(t)}{dt} \quad (4)$$

Substituting Eq.(3) and Eq.(4) into Eq.(2), we obtain the apparent permeability at a given mean pressure P_m :

$$K_{app} = \frac{\mu_0 V_{ch} L}{2 A_s P_m} \left| \frac{d \ln(P_1 - P_2)}{dt} \right| \quad (5)$$

As a corollary, we deduce that the isothermal assumption is verified if the variations of $\ln(P_1 - P_2)$ as a function of time are linear. These variations are represented in Fig. 6 for the track-etched polycarbonate membrane at $P_m = 34$ mbar, for the Norway spruce in the longitudinal direction at $P_m = 50$ mbar and in the tangential directions at $P_m = 471$ mbar.

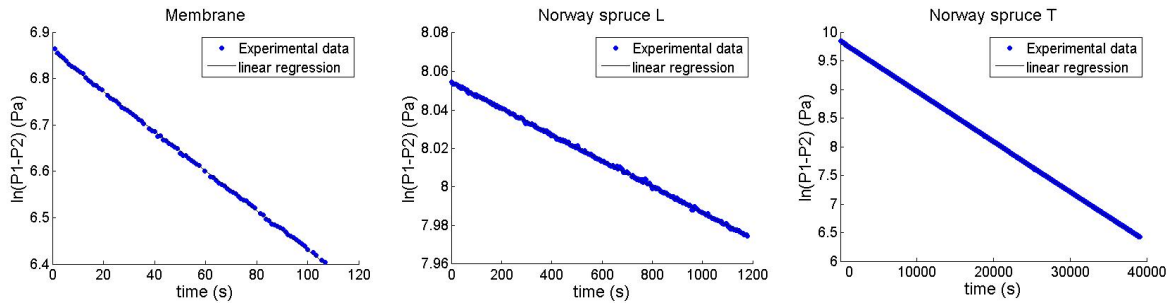


Figure 6: Variations of $\ln(P_1 - P_2)$ as a function of time and associated linear regression: track-etched polycarbonate membrane (left) and Norway spruce in the longitudinal (center) and tangential (right) directions.

It appears that for the examined porous materials, the variations of $\ln(P_1 - P_2)$ as a function of time are actually linear, which demonstrates that relaxation occurs in isothermal regime. Thus the apparent permeability at the mean pressure P_m can be easily deduced from the slope of the $\ln(P_1 - P_2)$ vs t curve.

From Fig. 6 and Eq. 5, we determined the apparent permeability of the track-etched membrane at 34 mbar, *i.e.* $K_{app} = 1.62 \cdot 10^{-15} \text{ m}^2$, the apparent permeability of Norway spruce in the longitudinal direction at $P_m = 50$ mbar, *i.e.* $K_{app} = 2.47 \cdot 10^{-13} \text{ m}^2$ and in the tangential directions at $P_m = 471$ mbar, *i.e.* and $K_{app} = 9.67 \cdot 10^{-18} \text{ m}^2$. It appears that the tangential permeability of Norway spruce is much lower than its longitudinal permeability. Indeed, as mentioned earlier, wood is highly anisotropic.

We performed the relaxation measurements at different mean pressures, for the polycarbonate track-etched membrane and the Norway spruce in longitudinal and tangential directions. The results are summarized in Fig. 7 where the apparent permeability is represented as a function of the reciprocal mean pressure.

It appears that the apparent permeability increases as the mean pressure decreases: this is due to molecular slip, this phenomenon becomes significant when the gas mean free path is of the order of the characteristic size of the wood microstructure. The corresponding Knudsen number ranges from 1.77 to 58.89 for the membrane, from 0.01 to 0.19 for the tracheid and from 0.44 to 14.70 for the bordered pits of Norway spruce in the longitudinal direction and from 0.01 to 0.02 for the tracheid and from 0.44 to 1.78 for the bordered pits of Norway spruce in the tangential direction. It should be noted that in the case of the bordered pits, the characteristic length used in the Knudsen number is the orifice diameter identified in the next section. For the pores of the track-etched membrane and for the Norway spruce tracheids, we use the values measured by SEM.

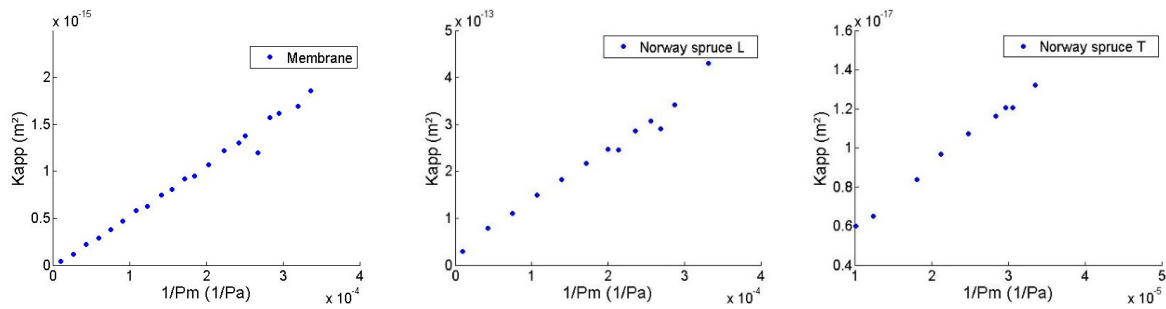


Figure 7: Apparent permeability K_{app} (m^2) as a function of the reciprocal mean pressure $1/P_m$ for the polycarbonate track-etched membrane (left) and the Norway spruce in the longitudinal (center) and tangential (right) directions.

4. PARAMETER IDENTIFICATION

The identification of effective pore diameters from variations of apparent permeability as a function of the mean pressure needs a prior assumption on the pore network. The network typically consists in elements such as pipes or orifices connected in series or in parallel. Its guess actually requires side information such as basic knowledge in wood anatomy for instance. The unknowns may be the connectivity of the network, the duct radius or orifice radius for example. The flow in each element is described by the appropriate model. The overall resistance of the pore network is deduced using the analogy between fluid flows and electric circuit (non-linear effects associated with contiguous pits for example are neglected). The unknowns are determined by minimizing the deviation between the experimental variations of the apparent permeability and the simulated ones.

4.1 Track-etched polycarbonate membrane

The porosity of the membrane consists in parallel identical cylindrical nanopores crossing the polycarbonate sheet. The gas flow in the nanopores was modelled by Beskok & Karniadakis pipe model [6]:

$$Q = -\frac{\pi D_1^4}{128\mu_0} \frac{dP}{dx} (1 + aK_n) \left[1 + 4 \frac{2 - \sigma}{\sigma} \frac{K_n}{1 - bK_n} \right] \quad (6)$$

where K_n is the Knudsen number (defined as $K_n = \lambda/R_1$ where λ is the mean free path, R_1 is the pore radius), D_1 is pore diameter, μ_0 is the gas dynamic viscosity of gas, a is a parameter depending on K_n , σ is the accommodation coefficient (we set $\sigma = 1$ for total accommodation) and b is an empiric parameter (b is set at $b = -1$ for slip flow).

Knowing the mean pore density as measured by SEM, *i.e.* $6.5 \cdot 10^{12}$ pores/ m^2 , we identified the membrane mean pore radius and found that it is equal to 38 nm. This is very close to the value measured by scanning electron microscopy, *i.e.* 35 nm.

We studied the effect of the accommodation coefficient σ on the results: the identified pore radius decreases from 38 nm to 27 nm when σ decreases from 1 to 0.5. Thus total accommodation seems a reasonable assumption.

It should be noted that we could not identify the mean pore density and the mean pore diameter together since in the available pressure range (from 30 mbar to 990 mbar), the gas flow regime in nanopores does not change: the flow remains in the transition regime.

4.2 Norway spruce

Finally, the present approach was used to characterize the multiscale porosity of Norway spruce. Petty [1] suggested a double porosity model where the tracheids and the bordered pits are connected in series as shown in Fig.7.

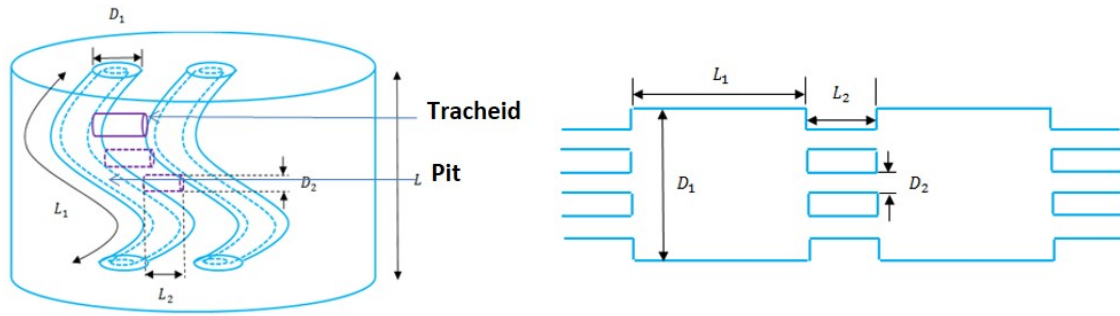


Figure 8: Schemes of Petty's double porosity model for softwood [1].

Gas flow in the tube-like tracheids was modelled by Beskok & Karniadakis's pipe model [6] and the throat-like pits by Borisov *et al.* orifice model [7]:

$$Q = \frac{D_2^2 \Delta P}{4P_m} \sqrt{\frac{\pi RT}{2M}} \xi_p^{ori} \quad (7)$$

where D_2 is the pit diameter, ΔP is the pressure drop across the pit, M is the gas molar mass and ξ_p^{ori} is a coefficient function of the Knudsen number.

We were not able to identify all the parameters of the pore network model. Thus we chose to fix the mean tracheid radius to the value measured by scanning electron microscopy, *i.e.* 11.7 μm , and to identify the mean pit radius and number of pits per tracheid. Identification was performed under full accommodation assumption. Permeability measurements in longitudinal and tangential led to the same value of the mean pit radius, *i.e.* 0.15 μm , but to different numbers of pits per tracheid, *i.e.* 3 pits/tracheid and 14 pits/tracheid, respectively. This difference is due to wood anisotropy. The obtained values are in reasonable agreement with the anatomical data reported in literature [8], *i.e.* 1-2 μm , and with the values measured by scanning electron microscopy, *i.e.* 0.7 μm . It should be noted that we also performed identification under partial accommodation assumption (α down to 0.5). Since two parameters are free instead of one in the case of the track-etched membrane, the effect of the accommodation coefficient on the parameters values is more complex. However, the order of magnitude is preserved (about 20 nm for the mean pit diameter, a few pits per tracheid in the longitudinal direction, between 14 and 20 pits per tracheid in the tangential direction).

5. CONCLUSIONS

1. An original experimental device was conceived and validated to measure a wide range of apparent-permeability, *i.e.* from 10^{-10} to 10^{-18} m^2 , at gas mean pressure ranging from 30 mbar to 2000 mbar.
2. Apparent-permeability measurements were performed on spruce wood in longitudinal and tangential directions: the anisotropic behaviour of wood was emphasized. Slip flow phenomena was observed at low gas pressure.
3. The identification method of morphological parameters was validated:
 - a. The identified mean pore radius of the track-etched membrane is close to the one measured by scanning electron microscopy.
 - b. For spruce wood, the mean pit radius and the number of pits per tracheid identified in tangential and longitudinal directions are in reasonable agreement with the anatomical data reported in the literature.

REFERENCES AND CITATIONS

- [1] Petty J.A. (1970). Permeability and structure of the wood of sitka spruce, *Proc. Roy. Soc. Lond.* **B175**, 149-166.
- [2] Redman, A. L., Bailleres, H., Turner I., & Perré, P. (2012). Mass transfer properties (permeability and mass diffusivity) of four australian hardwood species, *BioResources*, **7**, 3410–3424.
- [3] Rasband W.S., ImageJ, U. S. National Institutes of Health, Bethesda, Maryland, USA, <http://imagej.nih.gov/ij/>, 1997-2014.
- [4] Béguin, L., Grassl, B., Brochard-Wyart, F., Rakib, M., & Duval, H. (2011). Suction of hydrosoluble polymers into nanopores, *Soft Matter*, **7**, 96-103.
- [5] Agoua, E., & Perré, P. (2010). Mass transfer in wood: Identification of structural parameters from diffusivity and permeability measurements, *Journal of porous media*, **13**, 1017-1024
- [6] Beskok, A., & Karniadakis G.E. (1999). A model for flows in channels, pipes and ducts at micro and nano scales, *Microscale Therm. Eng.*, **3**, 43–77.
- [7] Borisov, S F, Neudachin, I G, Porodnov, B T, & Suetin, P E (1973). *Zh. Tekhn. Fiz.*, **43**, 1735 (in Russian)
- [8] Brändström J. (2001). Micro- and ultrastructural aspects of Norway spruce tracheids: a review, *IAWA Journal*, **22** (4), 333-353